Molecularly Engineered Flame Retardant Composite at Ultra-Low Loading Enables Safe PDOL Electrolyte for Solid-State Li Metal Batteries

Xiaobin Chen[a‡], Sili Qiu[a‡], Dazhu Chen[a], Chen Liu[a]*

Experimental section

1. Preparation of Ionic Liquid [TBP][BF_4]

The ionic liquid [TBP][BF_4] was prepared via an anion exchange method. First, sodium tetrafluoroborate and tetrabutylphosphonium bromide were used as reactants in an equimolar ratio, with deionized water as the solvent, to prepare a 0.25 mol L^{-1} solution. The reaction was carried out under constant temperature magnetic stirring at 30°C for 24 h to ensure complete reaction. After completion, dichloromethane (DCM) was added for extraction and separation. The organic phase was collected, and the solvent was removed via rotary evaporation. The product was then dried under vacuum at 60°C for 12 h to remove residual DCM, yielding a white crystalline [TBP][BF_4] with a yield of 80%. The prepared ionic liquid was transferred to a glove box to remove residual moisture and stored for later use, hereafter referred to as IL (Ionic Liquid).

2. In-Situ Preparation of Composite Flame-Retardant Modified PDOL-Based Electrolytes and Battery Assembly

All chemical reagents and battery consumables used in the experiments must be stored in an argon-filled glove box, and all battery preparation operations must also be carried out entirely within the glove box. The argon glove box maintains an O_2 content ≤0.1 ppm and an H_2O content ≤0.01 ppm.

2.1. Preparation of Precursor Solutions

The initiator ($InCl_3$), lithium salt (LiTFSI), APP, and IL were added to a reaction vessel in the proportions specified in Table S1. Liquid DOL monomer was then injected, and the mixed solution was stirred magnetically (500 rpm, 60 min) to form

a homogeneous solution, yielding precursor solutions DIA, DA, DI, and DOL. These correspond to the composite flame-retardant-modified (PDIA), single APP-modified (PDA), single IL-modified (PDI), and unmodified (PDOL) electrolyte systems, respectively.

In summarize, the PDOL-based electrolyte incorporating the composite flame retardant (APP + IL) was named PDIA, while the electrolytes incorporating a single flame retardant (either APP or IL) were named PDA or PDI, respectively. The electrolyte without any flame retardant was referred to as PDOL, and the liquid electrolyte without initiator was called DOL.

2.2. Battery Assembly

(1) LFP/SPE/Li Full Battery

The full battery was assembled by stacking components in the following order: positive electrode case → 0.5 mm stainless steel (SS) → LFP cathode → 25 μL precursor solution → PP separator → 25 μL precursor solution → Li anode → 0.5 mm SS → negative electrode case. After sealing with a coin cell sealer, the battery was left to stand for 12 h to ensure complete polymerization of DOL.

(2) Li/SPE/Li Symmetric Battery

For the lithium symmetric battery, the lithium metal anode replaced the cathode, and all other assembly steps were identical to those of the full battery.

Table S1. Composition in weight percent of different pDOL-based electrolytes (wt%)

	DOL	LiTFSI	APP	IL	$InCl_3$
PDIA	76.67	20.67	1.15	1.15	0.36
PDA	76.67	20.67	2.3	0	0.36
PDI	76.67	20.67	0	2.3	0.36
PDOL	78.48	21.15	0	0	0.37

Characterizations

The SEM morphologies of the electrolyte membrane and cycled Li electrode surfaces were investigated by using a Hitachi SU-70 with an embedded EDS system. FTIR spectra were collected with a Nicolet 6700 instrument to study the IL and electrolytes. XPS spectra were generated by a ESCALAB 250Xi to analyze the element environment on the surfaces of cycled Li electrodes, which were disassembled from Li//Li cells in a glove box with oxygen and water levels below 0.1 ppm. Raman spectroscopy was implemented through a RENISHAW via a Raman Microscope. Bruker EST's AVANCE III HD 500 MHz spectrometer was utilized to conduct NMR tests on the polymerization status of the polymer electrolyte. The polymerization status of the electrolyte matrix was analyzed using gel permeation chromatography (GPC) with a Waters E2695 instrument. The testing conditions involved tetrahydrofuran (THF) as the eluent, and the test solution was filtered through a microporous filter membrane prior to analysis. XRD analysis of the crystallinity of the polymer electrolyte was conducted using a Miniflex 600 device from Rigaku Corporation. DSC measurements were conducted within a temperature range of −90 to 100 °C at a heating rate of 5 °C min^{-1} by a DSC 25, TA Instruments. The thermal stability was evaluated by TGA, using a TGA 55, TA Instruments under a N_2 flow at a heating rate of 5 °C min^{-1}, covering a temperature range of 30–700 °C.

Electrochemical measurements

The ionic conductivity was tested by using a coin cell which structure was stainless steel | composite electrolytes | stainless steel in the frequency range of 3 MHz to 1 Hz with an oscillation amplitude of 10 mV under the temperature range between 70 ℃ and 25 ℃. The ionic conductivity σ was calculated based on the following equation:

$$\sigma = {}^{l}/_{RS}$$

where l represents the thickness of the electrolyte membrane, R is the bulk

resistance of electrolytes, and S refers to the contact area between electrolyte and electrode.

The linear sweep voltammetry was tested by using a Li | composite electrolytes | stainless steel coin cell under 30 °C, and the range of potential was from 0 V to 6 V at a scan rate of 0.5 mV s^{-1}. A symmetric coin cell of Li | composite electrolytes | Li was used for both the tests of lithium ion transference number, Tafel curves and interfacial stability of the composite electrolytes against lithium electrode. The galvanostatic cycling was conducted at a current density of 0.1 mA/cm^{-2} with charging and discharging for 1 h, respectively.

Battery cycling tests

The charge/discharge cycling performance was tested using $LiFePO_4$//Li and NCM811//Li full cells under 0.2 C at 30 °C. The entire assembly was packaged under a pressure of 5 MPa to ensure proper contact between the electrodes and electrolyte. The cycling tests for $LiFePO_4$//Li full cells were conducted with cutoff voltages set at 2.5 V for charging and 4.0 V for discharging, corresponding to a theoretical capacity of 174 mAh g^{-1}. For NCM811//Li full cells, cycling tests were conducted with cutoff voltages set at 2.8 V for charging and 4.2 V for discharging, corresponding to a theoretical capacity of 220 mAh g^{-1}. The above detailed parameters are summarized in Table S2.

Table S2. Charge-discharge cycling protocol for full cells

	Rate	Cutoff voltages	Theoretical capacity	Temperature	Packaged pressure
$LiFePO_4$//Li	0.2 C	2.5 V-4.0 V	174 mAh g^{-1}	30°C	5 MPa
NCM811//Li		2.8 V-4.2 V	220 mAh g^{-1}		

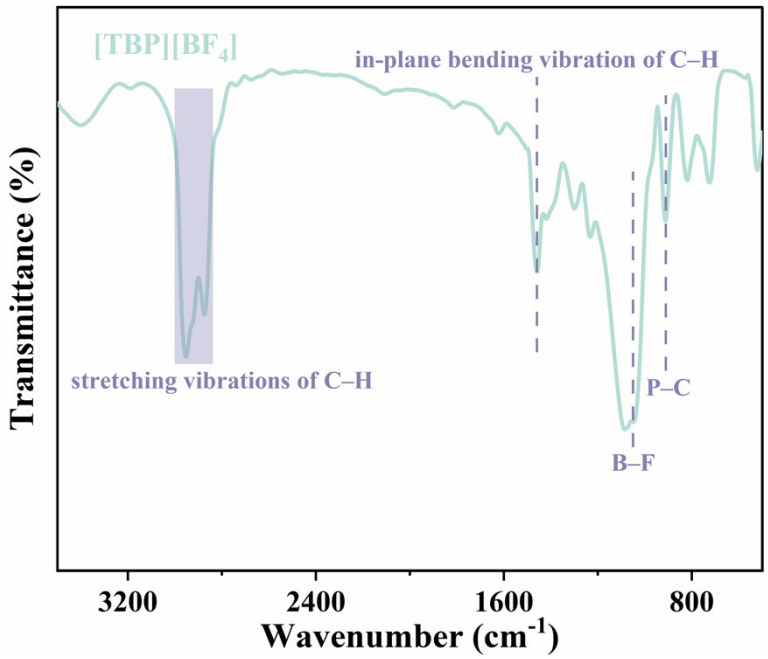

Fig. S1 FTIR spectra of [TBP][BF_4].

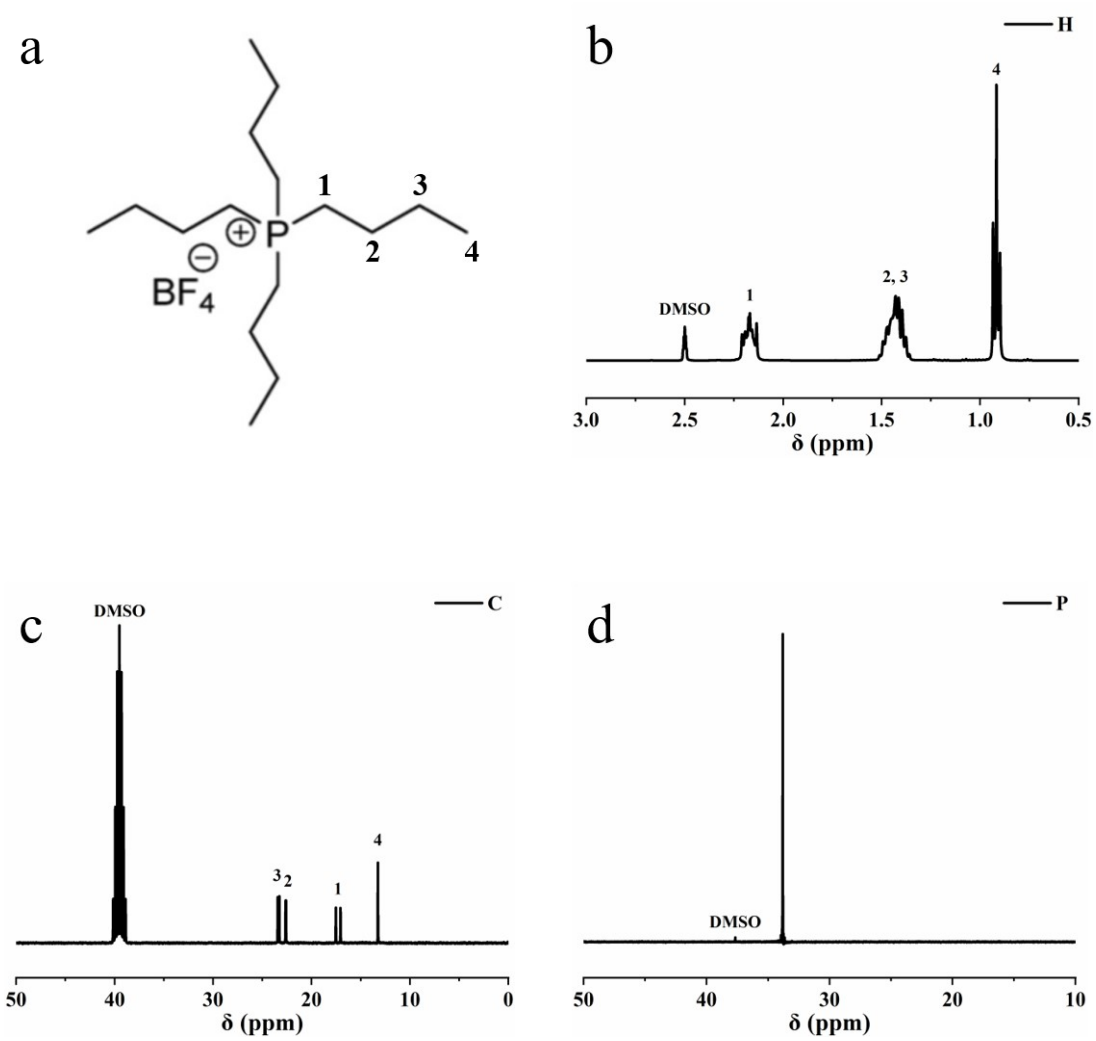

Fig. S2 (a) Schematic diagram of the molecular structure of [TBP][BF_4]. (b) ^{1}H NMR spectra of [TBP][BF_4]. (c) ^{13}C NMR spectra of [TBP][BF_4]. (d) ^{31}P NMR spectra of [TBP][BF_4].

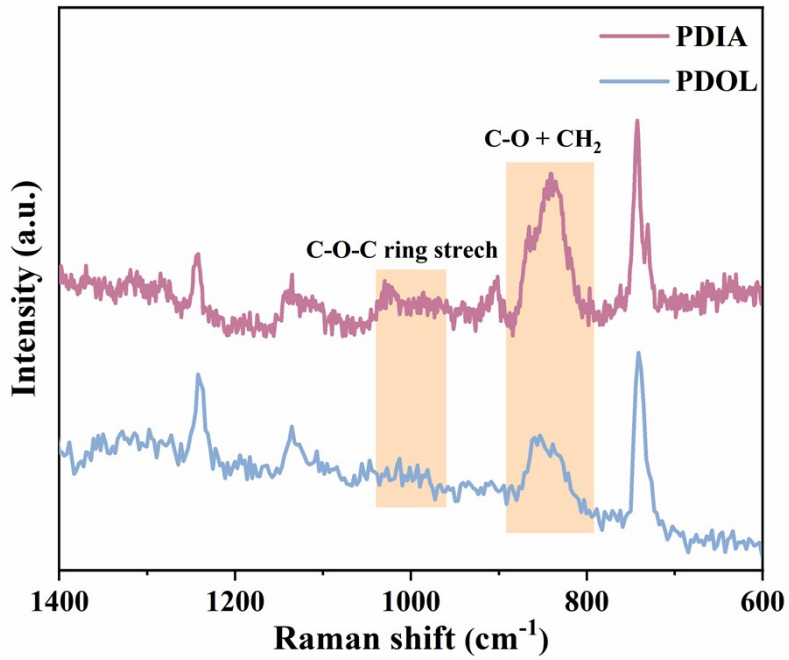

Fig. S3 Raman spectra, (d) ^{1}H NMR spectra and (e) XRD patterns of PDIA and PDOL.

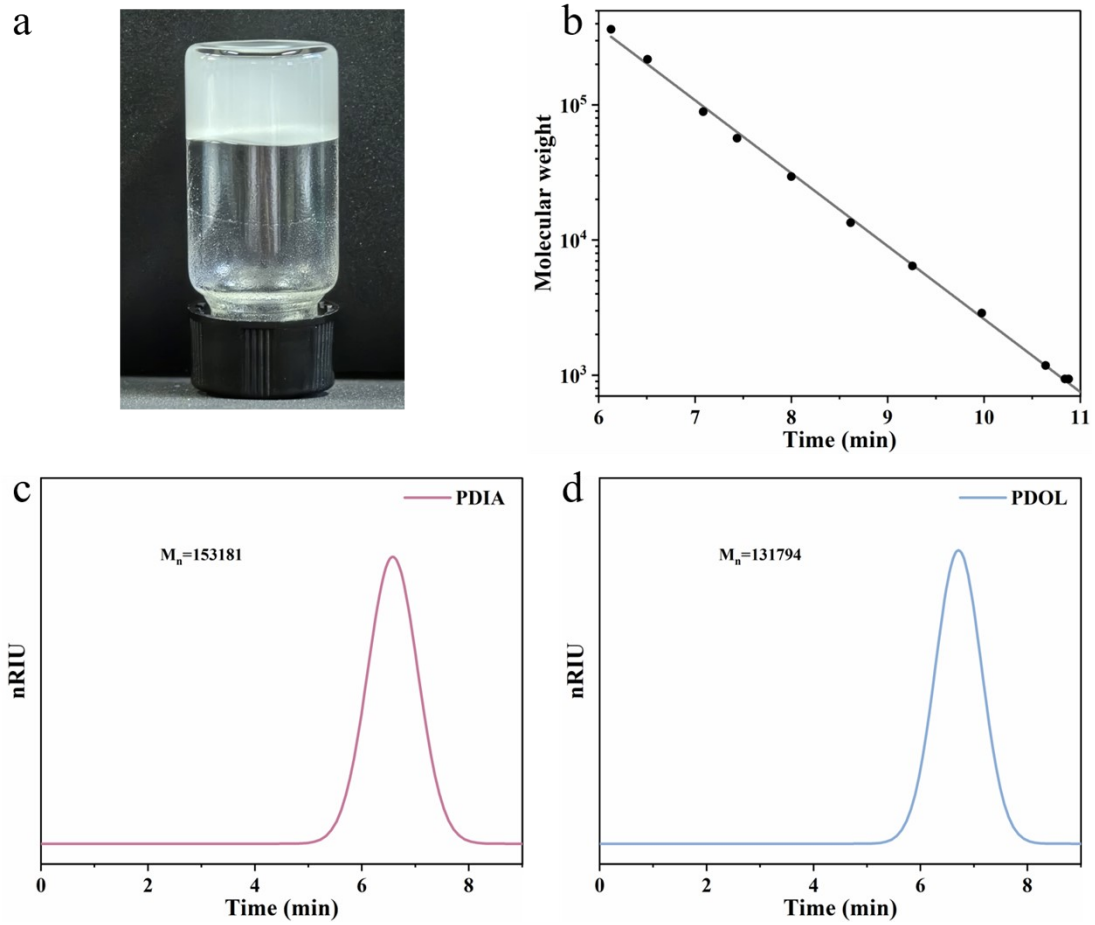

Fig. S4 (a) Optical image of the PDIA precursor solution after polymerization. (b) Correlation curve between retention time and polymer molecular weight from GPC tests. GPC test concentration-elution time curves: (c) PDIA, (d) PDOL.

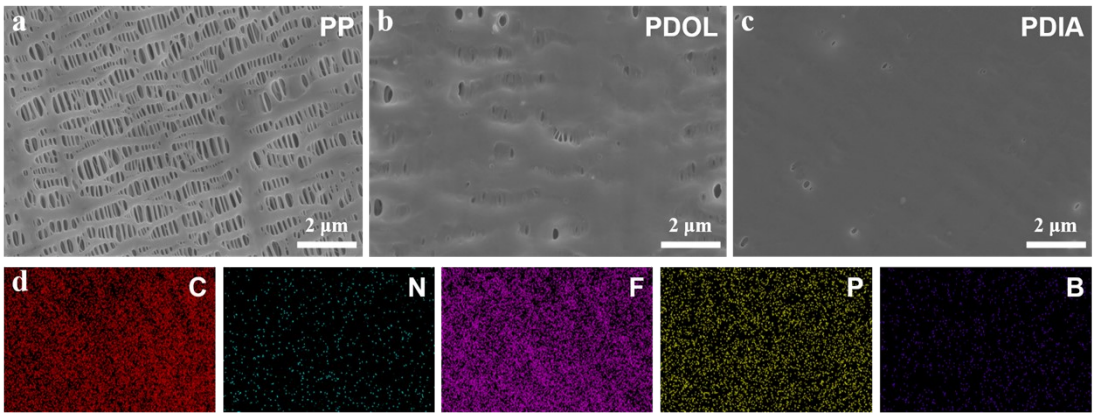

Fig. S5 SEM morphology characterization of (a) PP separator, (b) polymer electrolyte PDOL and (c) polymer electrolyte PDIA. (d) EDS element mapping images of PDIA.

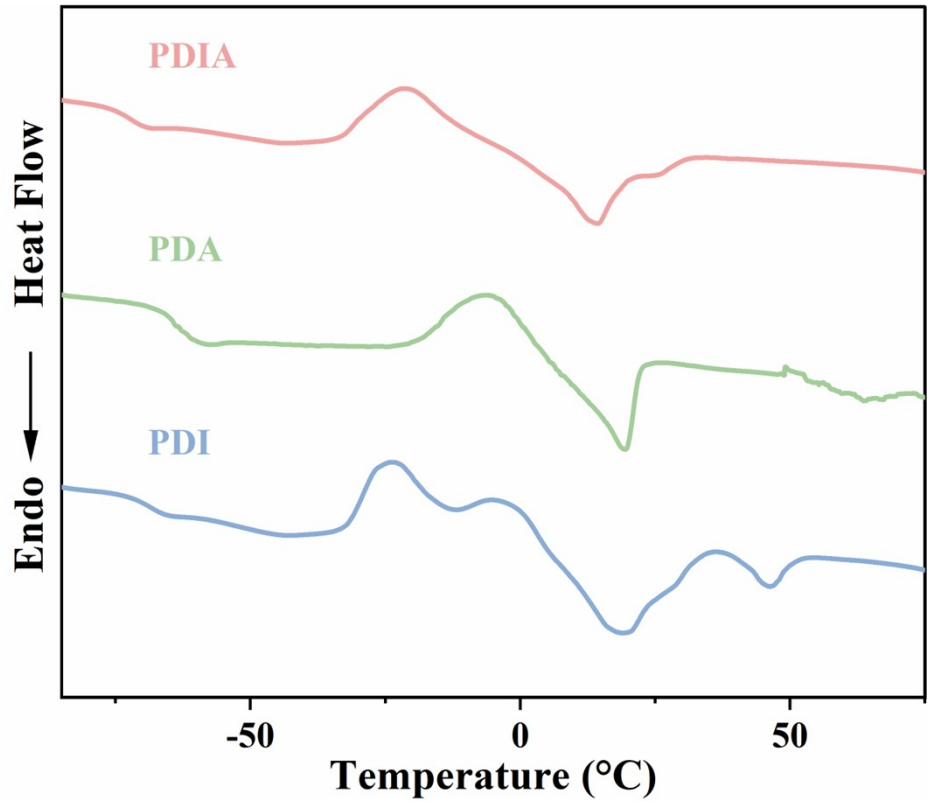

Fig. S6 DSC of PDIA, PDA and PDI.

Table S3. Quantified data of TGA and DTG for PDIA, PDA, and PDI electrolytes

	T_{onset} (°C)	DTG peak temperature (°C)		Residue (%)	n
		Peak 1	Peak 2		
PDIA	100.6 ± 1.1	138.4 ± 1.2	449.5 ± 0.9	2.3 ± 0.6	
PDA	91.1 ± 0.8	120.4 ± 1.0	416.4 ± 1.1	2.4 ± 0.5	3
PDI	94.2 ± 1.0	121.7 ± 1.2	422.2 ± 0.7	2.4 ± 0.8	

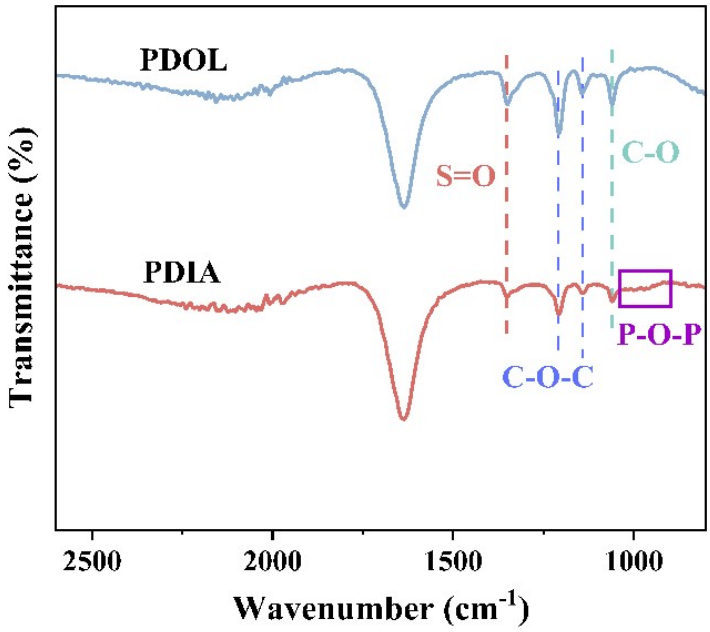

Fig. S7 The FTIR spectra of TGA residues at 410 °C from PDOL and PDIA electrolytes.

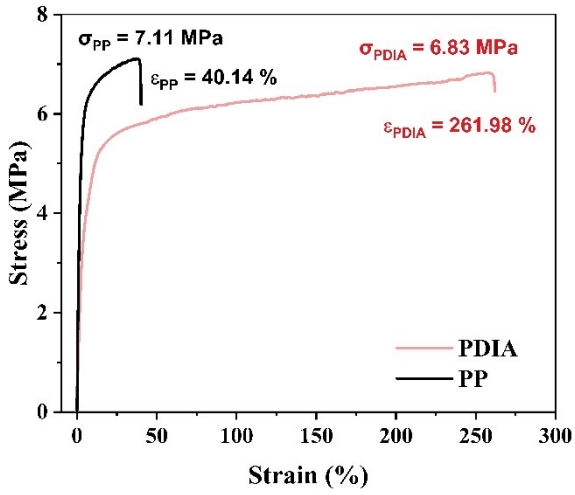

Fig. S8 Stress-strain curves of PDIA membrane and PP separator.

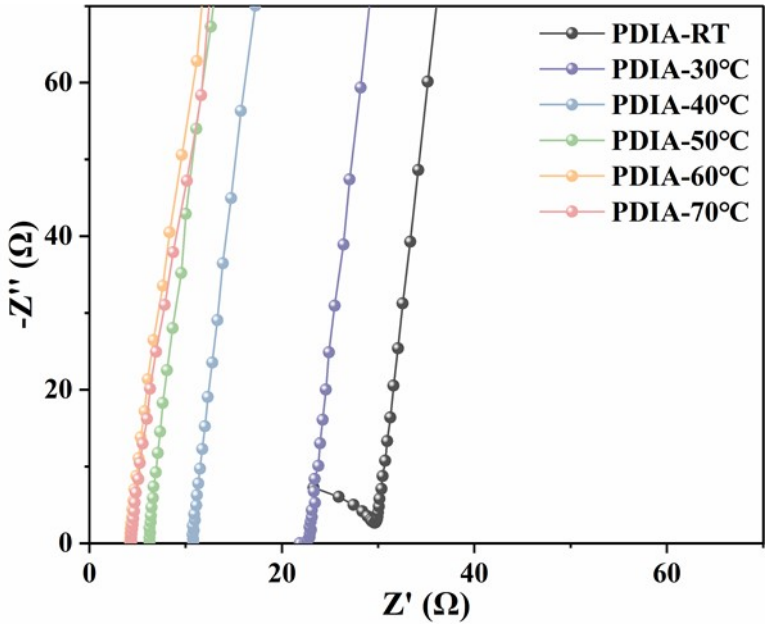

Fig. S9 Nyquist plots for different temperature of PDIA.

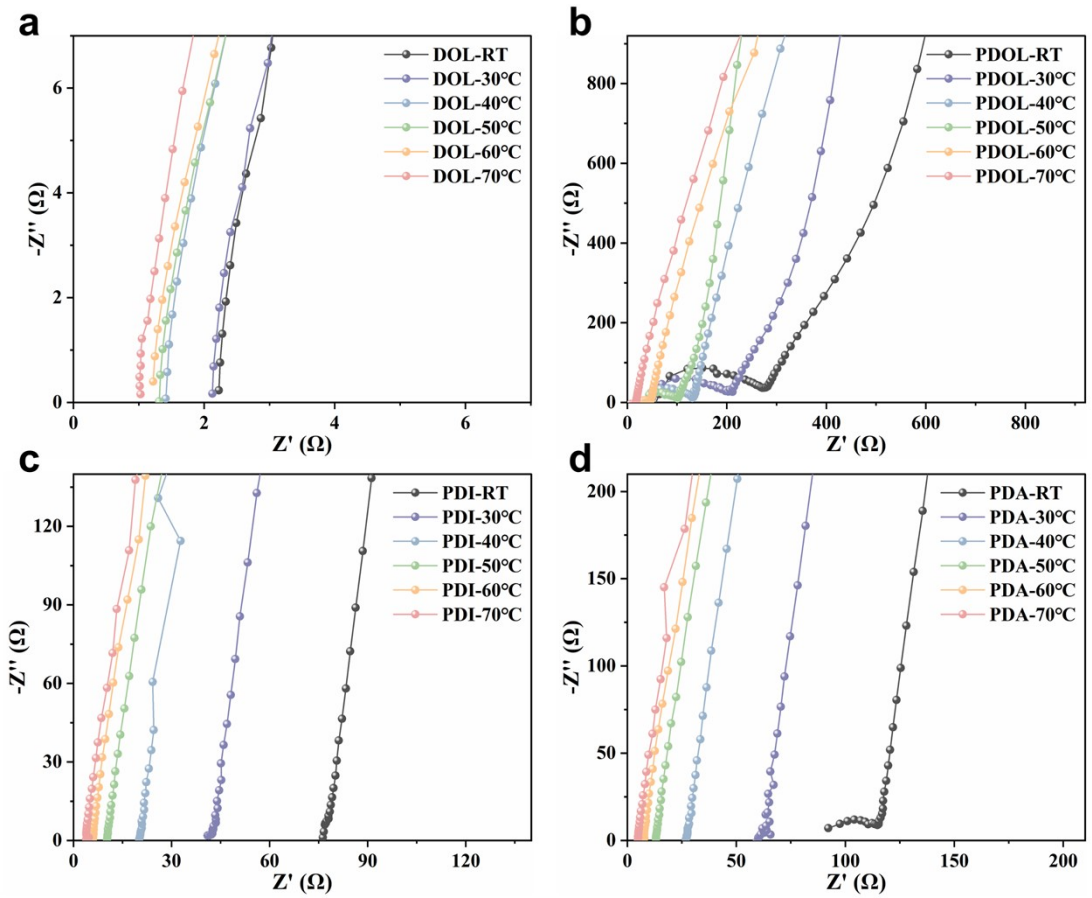

Fig. S10 Nyquist plots for different temperature of (a) DOL, (b) PDOL, (c) PDI and (d) PDA.

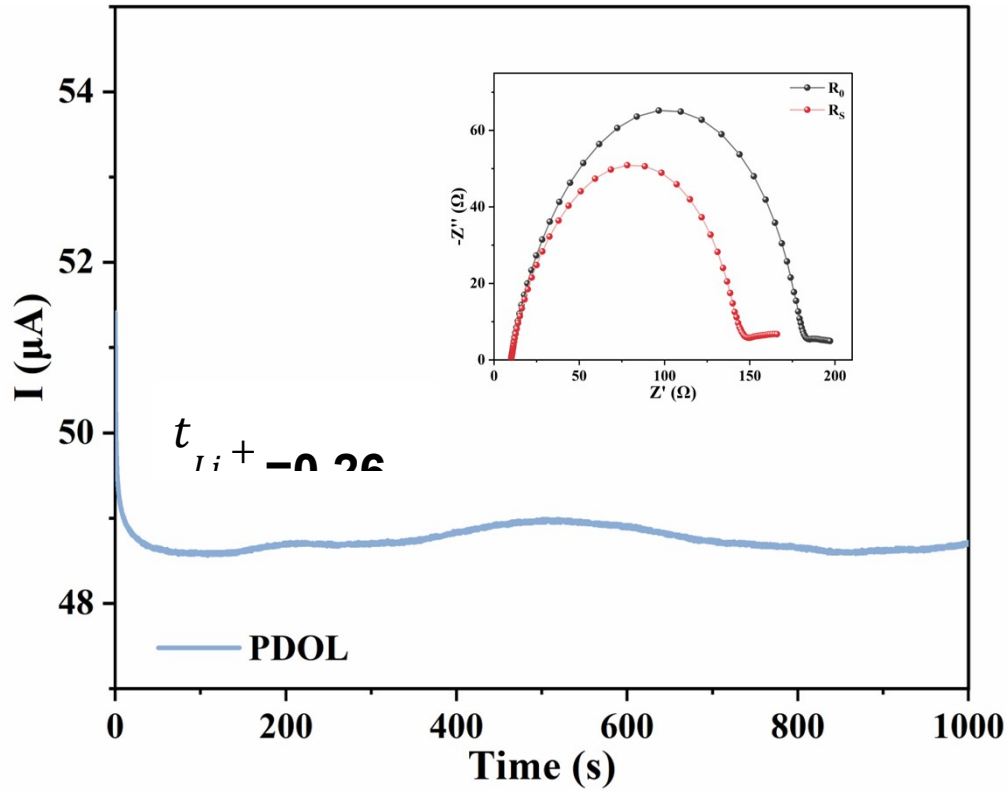

Fig. S11 Chronopotentiometry curve and impedance curves of PDOL.

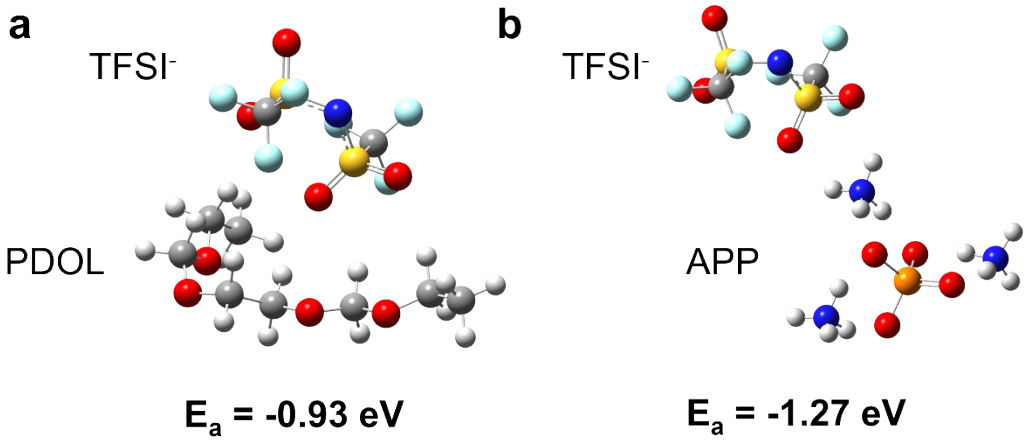

Fig. S12 Absorption energy of $TFSI^-$ with (a) PDOL, and (b) APP.

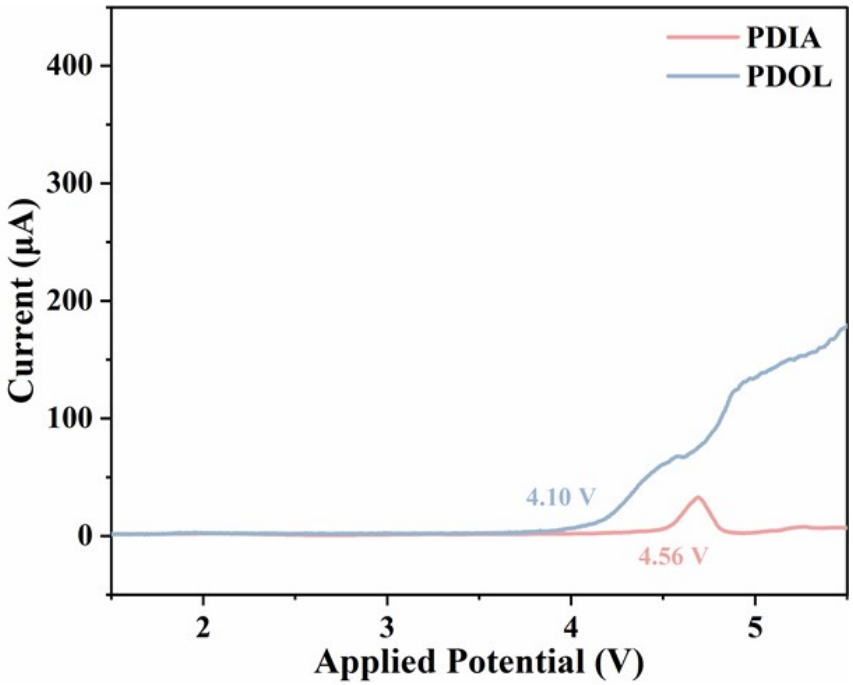

Fig. S13 Linear sweep voltammetry (LSV) curves of PDIA and PDOL.

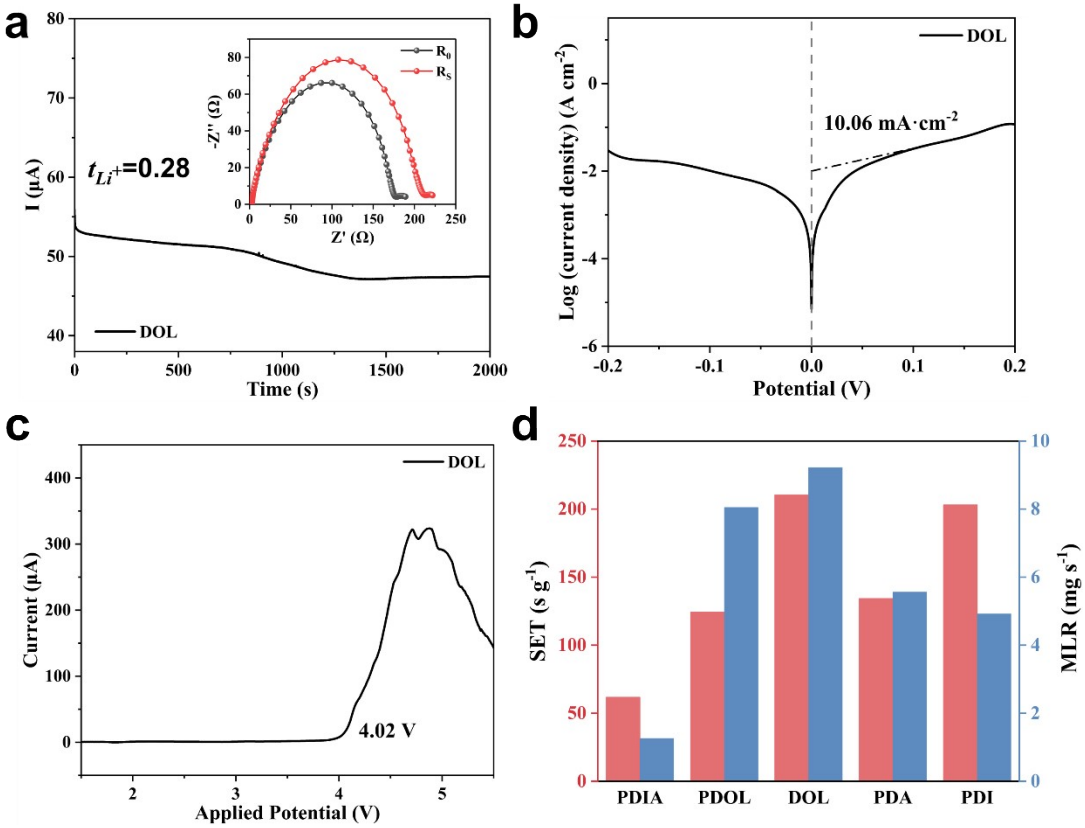

Fig. S14 (a) Chronopotentiometry curve and impedance curves, (b) Tafel plots, and (c) LSV curve of DOL electrolyte at room temperature. (d) The comparation for different DOL-based electrolytes.

Table S4. Electrochemical performance and flammability for different electrolytes

	σ (S cm^{-1})	t_{Li}^+	I_0 (mA cm^{-2})	Electrochemical window (V)	SET (s g^{-1})	MLR (mg s^{-1})
PDIA	1.47×10^{-4}	0.60	28.38	4.56	17.78	1.26
PDOL	7.97×10^{-6}	0.26	2.70	4.10	124.71	8.05
DOL	9.96×10^{-4}	0.28	10.06	4.02	210.32	9.22
PDA	1.90×10^{-5}				90.21	5.56
PDI	2.90×10^{-5}				122.22	4.92

Additionally, as shown in Fig. S14 and Table S4, the neat liquid DOL sample exhibits similar t_{Li}^+ and higher i_0 compared to the polymerized PDOL electrolyte. This can be attributed to its higher fluidity as a liquid electrolyte, which facilitates faster ion conduction. However, the relatively poor chemical stability of neat DOL result in a narrow electrochemical window when compared to PDOL.

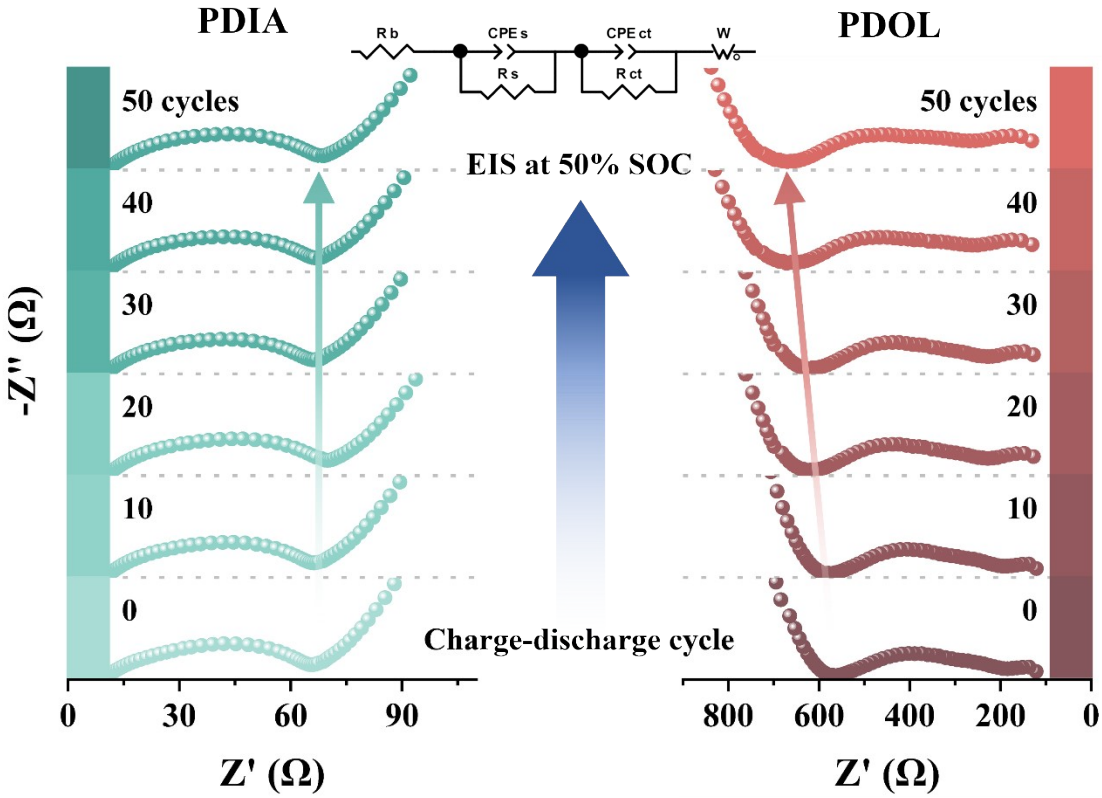

Fig. S15 Nyquist plots and equivalent circuit of LFP//Li cells at 50 % SOC for each 10 cycles based on PDIA and PDOL electrolytes.

Table S5. The values of R_s and R_{ct} of LFP//Li cells based on PDIA and PDOL electrolytes for each 10 cycles

	LFP/PDIA/Li	LFP/PDOL/Li	Cycle
R_s (Ω)	52.85	271.47	0
	52.34	288.60	10
	56.13	307.18	20
	51.43	324.49	30
	53.63	329.06	40
	54.56	337.05	50
R_{ct} (Ω)	26.62	290.80	0
	27.88	247.66	10
	29.14	253.41	20
	28.31	266.14	30
	27.75	282.14	40
	28.49	286.58	50

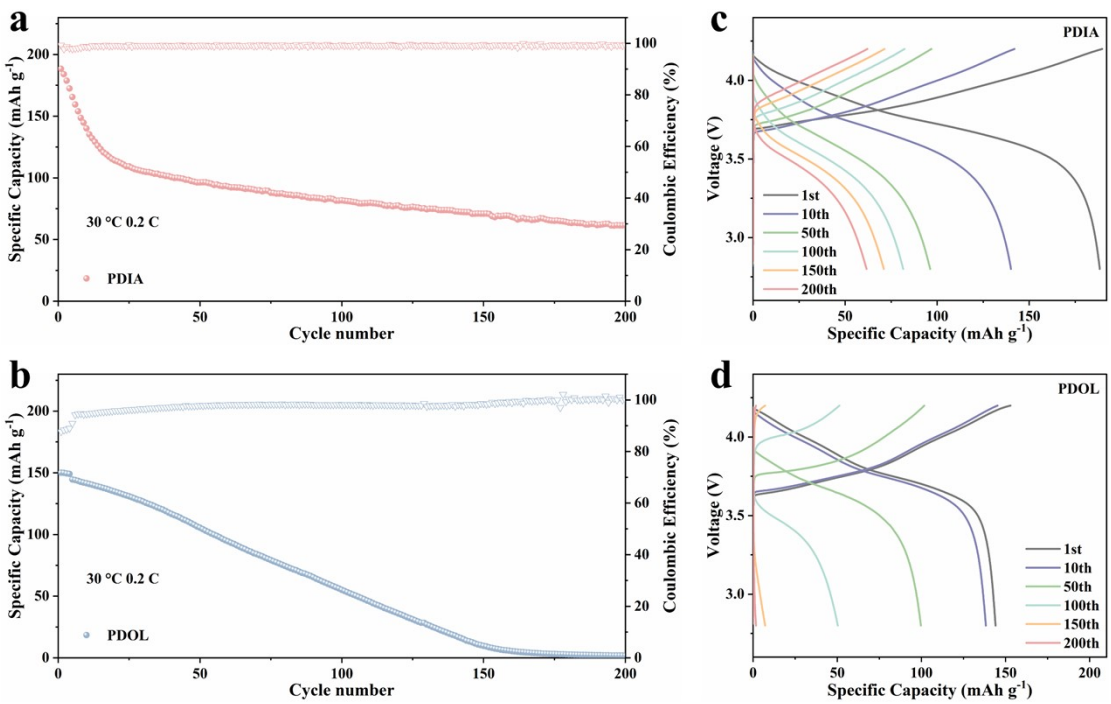

Fig. S16 Long cycle performance of NCM811 cells assembled with (a) PDIA and (b) PDOL at 30 °C and rate of 0.2 C. The corresponding specific capacity-voltage curves during charge-discharge processes for (c) PDIA and (d) PDOL, respectively.

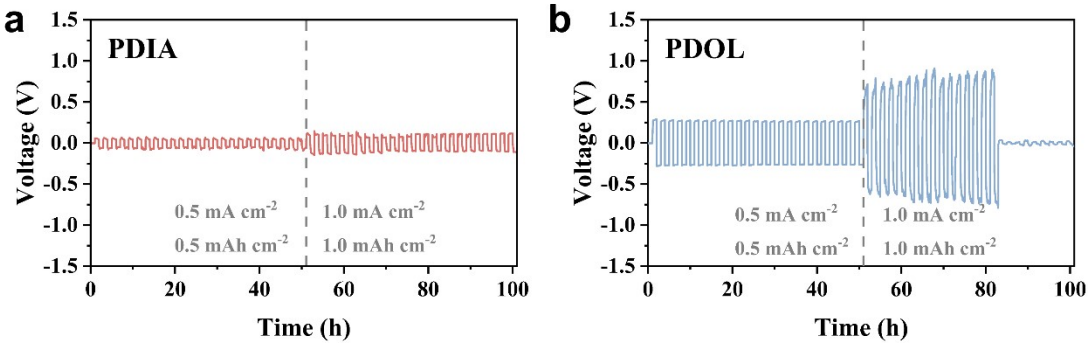

Fig. S17 The potential profiles of Li/Li symmetric batteries with (a) PDIA, and (b) PDOL at 0.5 to 1.0 mA cm^{-2} under 30°C.

Specifically, the PDIA cell maintains polarization voltages of approximately 60.3 mV at 0.5 mA cm^{-2} and 113.1 mV at 1.0 mA cm^{-2}, with no significant signs of voltage fluctuations or short-circuit behavior. In sharp contrast, the PDOL-based cell shows poor interfacial stability under the same operating conditions. At 0.5 mA cm^{-2}, a large polarization of ~267.9 mV is observed, and when the current density increases to 1.0 mA cm^{-2}, the polarization rapidly escalates from 718.2 to 908.5 mV, followed by an abrupt voltage drop indicative of dendritic penetration and internal short circuit. These results confirm that the PDIA electrolyte enables substantially enhanced Li metal stability under practical high-rate conditions, whereas PDOL suffers from severe interfacial degradation and dendrite-induced failure.

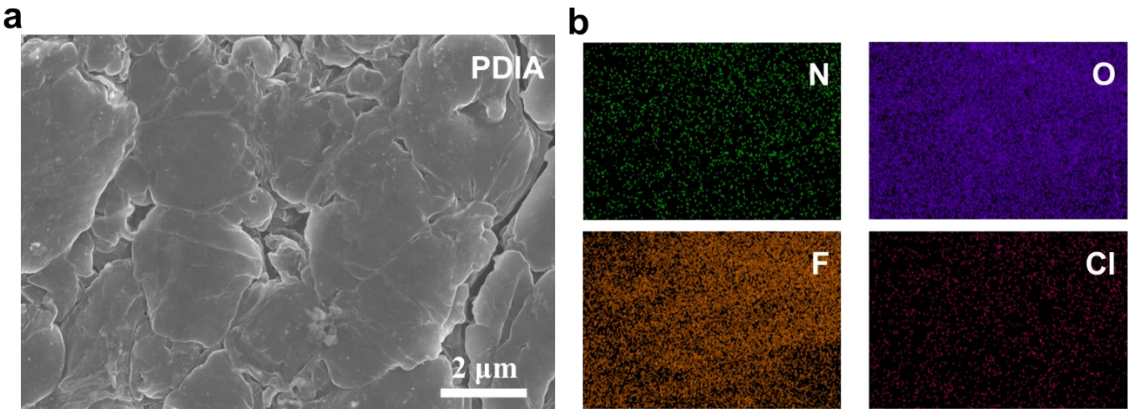

Fig. S18 (a) SEM images of the surface of cycled lithium electrodes of PDIA lithium symmetric battery. (b) EDS elemental mapping of the cycled lithium electrode of Li/PDIA/Li.

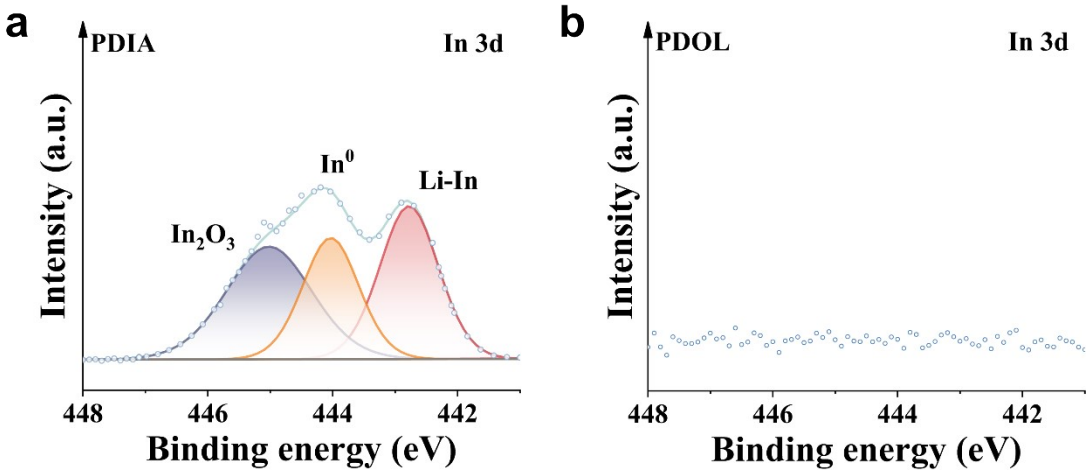

Fig. S19 XPS spectra of In 3d taken from cycled Li metal surface with (a) PDIA, and (b) PDOL.

As shown in Figure S19a, the XPS spectra show the presence of In signals in the PDIA sample, which is originated from $InCl_3$ used as the initiator. In contrast, no such signals appear in the PDOL (Figure S19b). This is because the addition of the composite flame retardant in PDIA enhances the mobility of the polymer chain segments (Figure. 2a), and subsequently carries trace In ions to move within the electrolyte, facilitating their contact with Li metal anode to form Li-In compounds. It is known that Li-In alloy can enhance overall ionic conductivity and stabilize the interface, leading to improved cycling performance and reduced polarization.[18] Although signals of In and In_2O_3 are present, their lower intensities indicate that their contribution to the electrochemical performance is smaller than that of the Li-In alloys.

Table S6. The combustion test results for different electrolytes

	Initial mass (mg)	Residual mass (mg)	Combustion time (s)	Mass loss rate (mg s^{-1})	SET (s g^{-1})
PDIA	9.00	8.80	0.16	1.26	17.78
PDA	9.10	4.50	0.83	5.56	90.21
PDI	9.00	3.60	1.10	4.92	122.22
PDOL	8.50	0	1.06	8.05	124.71

The self-extinguishing times (SET) were further evaluated by the equation of SET = t/m_i, where t and m_i are the burning time after ignition and the initial mass of the electrolyte membrane. According to a criterion for flame-retardant polymer materials, an SET value below 20 s g^{-1} is generally classified as flame-retardant. As listed in Table S4 and S6, the SET value of 17.78 s g^{-1} for PDIA is much lower than those of other samples (90.21 s g^{-1} for PDA, 122.22 s g^{-1} for PDI, 124.71 s g^{-1} for PDOL and 210.32 s g^{-1} for neat liquid DOL).